Chapter 2 Fractional Calculus Based PID Controllers`

2.1 Introduction

In recent decades, the response of a Fractional Order Proportional Integral Derivative (FOPID) controller has become a subject of interest for many researchers. From literature, it is observed that numerous studies are conducted to understand the behavior of FOPID under various operational configurations. Although promising results have been attained using the FOPID controller, it is observed that the dimensional aspects associated with it have been overlooked so far. In this regard, the present study is emphasized to develop a new FOPID controller, which is dimensionally balanced. It is introduced as a dimensionally balanced fractional order proportional integral derivative controller (DBFOPID). The proposed controller has been tested on an isolated and two area electrical power systems. Furthermore, the optimized parametric values of the variables affecting overshoot, settling time and rise time are estimated using Particle Swarm Optimization (PSO). To evaluate the optimum values of these parameters, integral of the time-weighted absolute error performance index has been used. The conventional Proportional Integral Derivative (PID) controller controlled Automatic Generation Control (AGC), and the proposed DBFOPID controller systems are compared. Further, the sensitivity of the system to human controllable parameters to mitigate frequency variations like overshoot, settling time and rise time are studied.

Most of the power systems are associated with interconnected control areas and load frequencies. Maintaining the frequency and inter-area tie power within the desired limits is an essential element in designing power systems. Additionally, generators must also be regulated continuously to monitor the power demand with the reactive generation else, the variation of voltages may exceed the desired limits.

2.2 Automatic Generation Control

In recent circumstances, large interconnected systems cannot be regulated manually, which made AGC as one of the essential components in most of the generators. AGC is the system utilized to control the output power of different generators at various power plants in response to load alterations. The preliminary properties of AGC are to monitor frequencies within the desired limits

and are especially used when there is a significant variance of load in the power system. AGC reduces operating costs by distributing generation optimally within the areas or units of power systems. Further, AGC perpetuates power interchanged among the control areas by altering the output of the chosen generators, and this process is called Load Frequency Control (LFC). The typical layout of AGC is shown in Figure 2.1.

The AGC's control actions can be classified into two loops, namely the primary loop and secondary loop. The primary loop, is also referred to as primary control, maintains electricity produced by load change. But due to the presence of steady-state error's offset in the primary loop, the secondary loop is much robust than the primary loop since steady-state error's offset results in a considerable fall in frequency. Further, the secondary loop not only eliminates the offset but also reinstates the set point of the system (Grainger *et al.* 2003).

In a single area electrical power system, AGC reinstates frequency to its original nominal value. Further, to stabilize the frequency deviations in single area power systems, a reboot action is installed using an integral controller, which enhances the system's type by slashing the final frequency deviation to zero.

In multi-area electrical power systems, the power networks are transmitted through tie-lines among the control areas. For sensitivity in all areas of power systems, tie-lines are used. One of the fundamental advantages of multiple area power systems is that in the case of an absolute unit failure, the remaining units help to reinstall frequency. Other uses of multi-area electrical power systems include optimal generation, reliability, cost-effective generators (Dorf and Bishop 2011). Numerous studies have been conducted on the fractional order (FO) controller for improving the stability and response of an AGC using multiple algorithms (Li *et al.* 2010; Luo *et al.* 2010; Padula and Visioli 2011; Shah and Agashe 2016b). Isolated and two area power system along with the FO controller are considered to improve the stability and response in AGC. For the purpose of optimizing the control design, Integral of the time-weighted absolute error (ITAE) (Alomoush 2010) is adopted widely as a performance index. The dominance of the FO controller over the classical IO controllers in context to AGC systems is also highlighted in subsequent sections.

From Figure 2.1, it is evident that Turbine, Voltage sensor and comparator, the Excitation controller, the Steam value controller and Generator are the component of a typical AGC system.

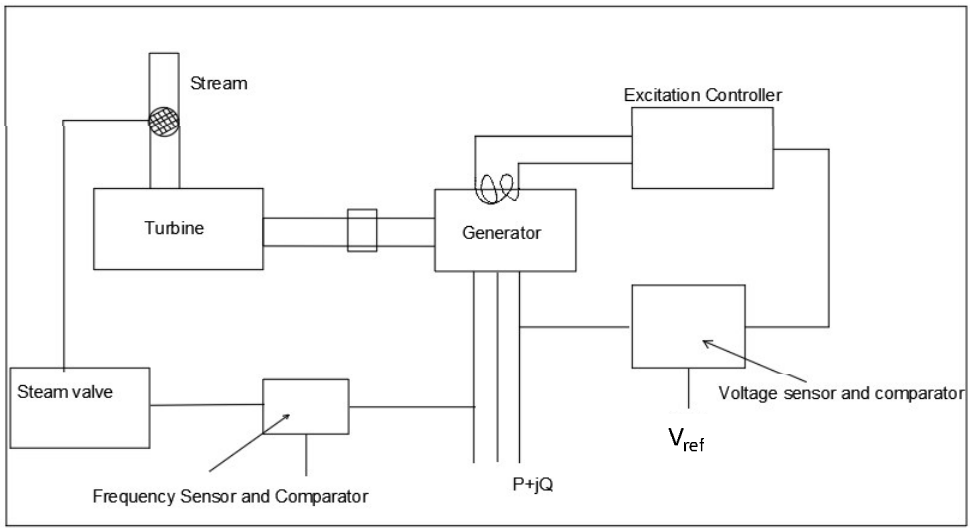

Figure 2.1 Typical layout of AGC System

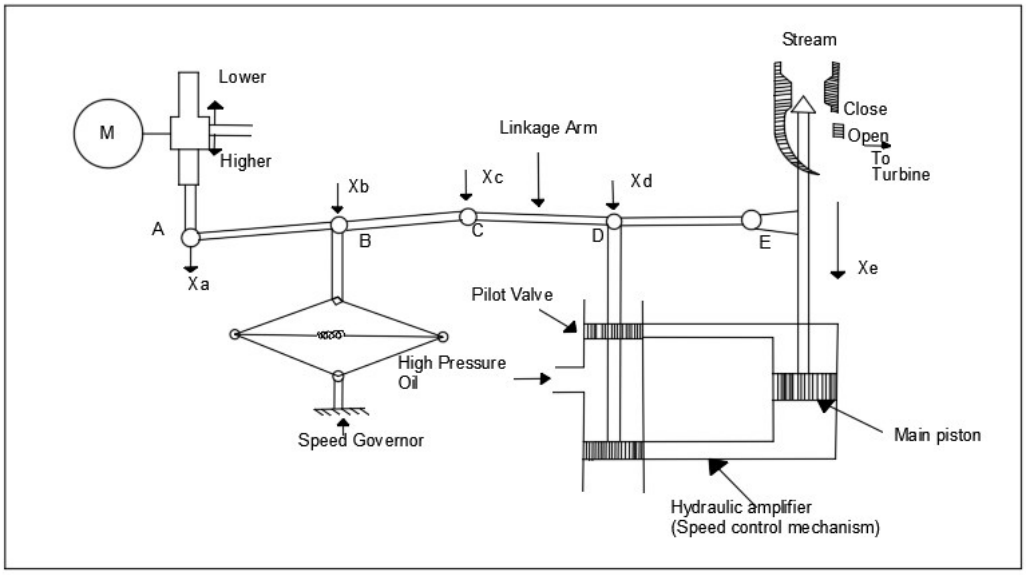

Figure 2.2. Turbine speed governing system

A deep insight into each component is presented in Figure 2.2. Furthermore, a feedback loop is also shown in Figure 2.2. AGC system inherently utilizes Proportional Integral (PI) and PID controllers to accelerate response dynamically. Besides abolishing or reducing the steady-state error, these controllers reduce steady-state error with a minimal settling time (Kundur 1994).

2.3 Basic Definitions of Control Theory

2.3.1 Transfer function

Transfer function synonymously known as a frequency domain, is a function that establishes the relation between output and input signals of any control system. It can be defined as the Laplace transformation ratios of output to input variable by assuming zero initial values.

Example: For a control system with continuous input time signal $x(t)$ and output time signal $y(t)$, the transfer function is $G(s)$ given by (2.1)

$$G(s) = \frac{Y(s)}{X(s)} \tag{2.1}$$

where, $Y(s)$ and $X(s)$ are Laplace transformations of $y(t)$ and $x(t)$ respectively.

2.3.2 Overshoot

Overshoot is the measure by which the control system exceeded the steady-state system target. For a given damping ratio $'\vartheta'$, the overshoot (percentage) can be evaluated by (2.2)

$$Overshoot\ (\%) = 100.\, e^{\left(\frac{-\vartheta\pi}{\sqrt{1-\vartheta^2}}\right)} \tag{2.2}$$

2.3.3 Rise time

The time required to overcome a predefined threshold of lower voltage to upper voltage for a signal is defined as rise time. The default percentages for lower and upper voltage thresholds are kept as 10% and 90% respectively. Elmore had given formulae to evaluate the rise time by (2.3)

$$Rise\ time = \sqrt{\frac{\int_0^\infty (t - t_d)^2 \dot{R_s}(t)dt}{\int_0^\infty \dot{R_s}(t)dt}} \tag{2.3}$$

where, R_s is the step-response and t_d is delay time of the control system.

2.3.4 Inertia constant

This constant is defined as the ratio of stored kinetic energy to the given generator at the synchronous speed.

2.4 Integer Order Proportional Integral Derivative Controller (IOPID)

Control theory is a branch of electrical engineering which deals with the property of dynamical systems, which is widely adopted by engineers and mathematicians. A control system can be defined as an instrument which instructs or regulates the actions/behavior of particular systems or

devices. The origin of formal introduction to control theory dates back to 1868, where Maxwell analyzed the dynamics of centrifugal governor in one of the research works entitled "On Governors" (Saadat 1999). The control theory was applied for testing of flights by Wright brothers and was able to control the dynamics of flights for significant periods of time. The safety of flight is highly dependent on the control of the plane. Since the introduction of control theory, many research works were evolved from control strategies to integrated open-loop control with genetic algorithms. The building blocks of control systems are called as control loops. Closed and open loops are two forms of control action which are classified based on the dependence on a process variable (PV). Any controller tracks PV with the reference set point.

Various mathematical and statistical techniques are utilized to analyze control systems. Further, numerous mathematical models and optimization techniques are used to mitigate frequency variations, which include overshoot, rise time and settling time. Based on past works in the literature review, the conventional PID controllers are ineffective for operating complex or nonlinear systems with hinder mathematical models. Hence an advanced integrated intelligent PID controller was introduced to tackle complex systems effectively. Subsequently, analyzing step-response characteristics has become a subject of interest with the introduction of fractional order control systems. PID controller is used in various industrial systems to minimize the error value, which occurs as a difference between the desired setpoint and a measured process variable. The parameters Proportional (P), Integral (I), and Derivative (D) are applied to alter the error value perpetually.

The words Integer order proportional integral derivative controller" (IOPID) and "PID" controller are used interchangeably. Attempts are made by the controller to minimize the error over time by adjustment of a control variable to a new value determined by a weighted sum, which can mathematically be represented by using (2.4).

$$u(t) = K_p e(t) + K_i \int_0^t e(\tau)d\tau + K_d \frac{de(t)}{dt} \tag{2.4}$$

where K_p, K_i and K_d all non-negative, denote the coefficients for the proportional, integral, and derivative terms respectively and the transfer function can be given by (2.5) and the block diagram is represented in Figure 2.3.

$$G_c(s) = K_p + \frac{K_i}{s} + K_d s \tag{2.5}$$

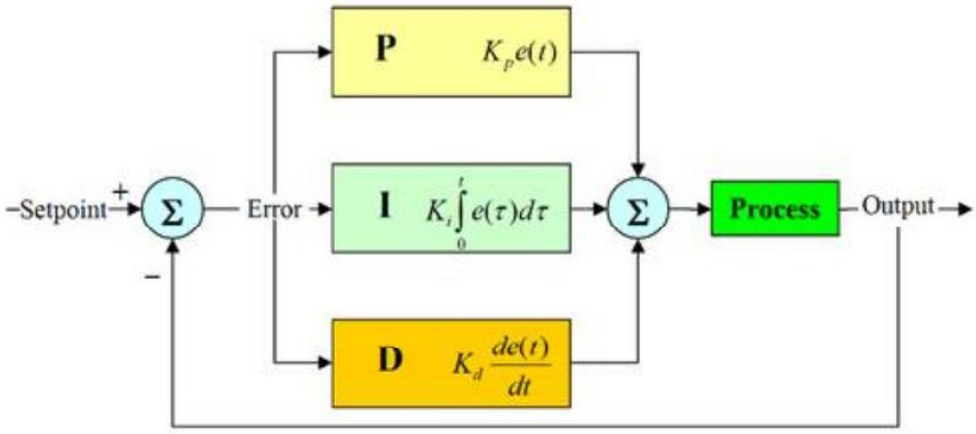

Figure 2.3. Architecture of PID controller

2.5 Fractional order PID Controller (FOPID)

Currently, fractional order controllers are extensively used in numerous works in view of the robust performance of a PID controller. Fractional order control systems such as FOPID controllers are used in various large scale industries due to its vast applicability and advantages in the field of engineering and technology. Due to memory property (Haldrup and Vera Valdés 2017) and inherit congenital properties, FOPID's have the edge over PID controllers. These inheritances of natural phenomena made these controllers applicable in areas such as energy systems simulations, robotics, chemical engineering, control and modeling of chaotic systems, regulation of hydraulic turbines, water networks, astronomy and other large scale industries (Algeria. et al. 2016). The fractional PID controller is introduced by Podlubny in 1994 for a fractional order system (Podlubny 1994). Subsequently, various other engineers designed fractional PID controllers using different designs and tuning methods (Shah and Agashe 2016b)

A fractional PID controller can typically be considered as an extension of the classical PID controller. The fractional order controllers are observed to be less sensitive to changes of the main concerns in the design of the controller. Numerous methods, including Ziegler-Nichols modified method, PSO, neural network, have been used in tuning PID controllers (Shah and Agashe 2016b). In contrast to the classical PID controller, fractional PID controller which is denoted by $PI^{\lambda}D^{\mu}$ has five parameters to tune, which facilitates to provide two more degrees of freedom in comparison with the conventional PID controller. The transfer function is given by (2.6)

$$G_c(s) = K_p + \frac{K_i}{s^{\lambda}} + K_d s^{\mu} \tag{2.6}$$

where λ and μ are order of fractional order integration and fractional order differentiation respectively with $0 < \lambda, \mu < 2$. In view of this, input to the system can be controlled by taking the following form (2.7)

$$u(t) = K_p e(t) + K_i J^{\lambda} e(t) + K_d D^{\mu} e(t) \quad (2.7)$$

2.6 Dimensionally Balanced Fractional Order PID Controller (DBFOPID)

The coefficient of integral and derivative K_i and K_d in the transfer function associated with FOPID, which is shown in (2.7) are expressed in fractional time $(time)^{-\lambda}$ and $(time)^{\mu}$ respectively while the dimension of K_i, K_d in PID controllers is $(time)^{-1}$ and $(time)^{1}$ as shown in (2.4). Therefore it is anticipated that the comparison of K_i and K_d in FOPID with K_i and K_d in PID controller is not mathematically consistent and credible. Owing to this fact, it can explicitly be concluded that the transfer function is not dimensionally balanced.

In view of this, considering the dimensional aspects, a new controller, Dimensionally Balanced Fractional Order PID controller (DBFOPID) is proposed in this study to remove the disparity in dimensions. This intended input function of the controller can be mathematically expressed as (2.8).

$$u(t) = K_p e(t) + (K_i)^{\lambda} D^{-\lambda} e(t) + (K_d)^{-\mu} D^{\mu} e(t) \quad (2.8)$$

The dimension of K_i and K_d in the proposed model is $(time)^{-1}$ and $(time)^{1}$ respectively which consistent with the dimension of K_i and K_d in PID controllers.

The transfer function is expressed as (2.9).

$$G_c(s) = K_p + \frac{{K_i}^{\lambda}}{s^{\lambda}} + {K_d}^{\mu} s^{\mu} \quad (2.9)$$

Therefore, this model will provide better and mathematically correct behavior of the control system and comparison of the results in the proposed model is mathematically justifiable with the PID controller.

2.7 Model Description of AGC for Isolated System

The objective of the AGC (Arya *et al.* 2011) is to keep the system frequency at a nominal level, i.e., to reduce the frequency deviation to zero. The equation of frequency set-point is given by

(2.10)

$$\Delta P_{ref} = -K_i \int \Delta f dt \tag{2.10}$$

The controller area error control (ACE) signal can be given as $\Delta\omega = \Delta f$.

Optimal value of K_i for the Integer order integral controller (IOI) is to be obtained by considering ITAE as a performance index. One of the major constraints is to determine the upper and lower limits of the controller constant. The mathematical model for the optimization problem can be presented as (2.11).

Minimize $ITAE(K_i)$

Subject to

$$K_i^{max} \geq K_i \geq K_i^{min} \tag{2.11}$$

Replacing IOI by DBFOPID controller whose transfer function is given by (2.9), the optimal values for DBFOPID controller constants K_p, K_i, K_d, λ and μ are obtained by solving the optimization problem (2.12):

Minimize $ITAE(K_p, K_i, K_d, \lambda, \mu)$

Subject to

$$K_p^{max} \geq K_p \geq K_p^{min}$$

$$K_i^{max} \geq K_i \geq K_i^{min}$$

$$K_d^{max} \geq K_d \geq K_d^{min} \tag{2.12}$$

$$\lambda^{max} \geq \lambda \geq \lambda^{min}$$

$$\mu^{max} \geq \mu \geq \mu^{min}$$

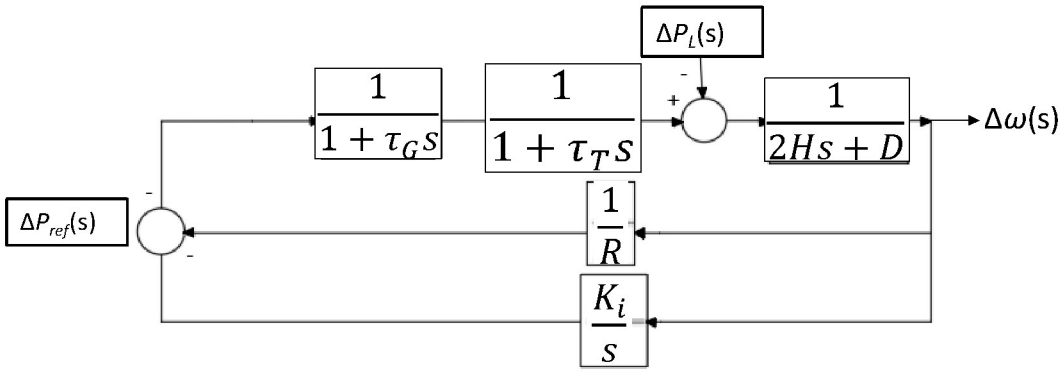

Figure 2.4. Block diagram of an AGC for isolated area system

In power systems, traditionally real power and reactive power systems are treated as separate systems, which are weakly coupled. Such a group of generators is said to be coherent. This lets the AGC loop represent the whole system and the group is called the control group. For an isolated system, during normal operation, the real power transferred over the tie lines. The block diagram representation of an isolated system can be given by Figure 2.4 and data is represented in Table 2.1.

Table 2.1: Data of AGC for an isolated system (Alomoush 2010)

Component	**Nomenclature**	**Values for Isolated system**	**Units**
Speed regulation	R	0.05	$\frac{Hz}{p.u.\ MW}$
Damping coefficient	D	0.06	$\frac{p.u.\ MW}{Hz}$
Inertia constant	H	5.00	$\frac{MWs}{MWA}$
Governor time constant	τ_G	0.20	s
Turbine time constant	τ_T	0.50	s
Base power	S_B	1000	MWA
Load change	ΔP_L	200	MW

2.8 Simulation Results for Isolated AGC system

The entire analysis which is carried out can be differentiated in three different cases, which are mentioned below.

Case 1: To exercise the optimized parametric values of K_p, K_i, K_d in case of PID controller.

Case 2: To investigate the optimized parametric values of K_p, K_i, K_d, λ and μ in case of isolated system configure with PID.

Case 3: To draw the optimized parametric values of K_p, K_i, K_d, λ and μ in case of system configure with DBFOPID.

At the outset of analysis, the first case where the isolated power system is configured with AGC

is simulated using MATLAB/Simulink®. PSO (Shah and Agashe 2016b), which is well known from the literature, is used to optimize the proportional, integral and derivative coefficients. The optimized K_p, K_i, K_d thus obtained, corresponding to this case are presented in Table 2.2. Similarly, the optimized set of values corresponding to K_p, K_i, K_d, λ and μ are evaluated for the rest cases and the results are tabulated in Table 2.2. For the comparison purpose, the frequency deviations with time in each of the cases are plotted in Figure 2.5. Few of the salient characteristics such as rise time, overshoot and settling time are observed for each of the cases and observations are tabulated in Table 2.2.

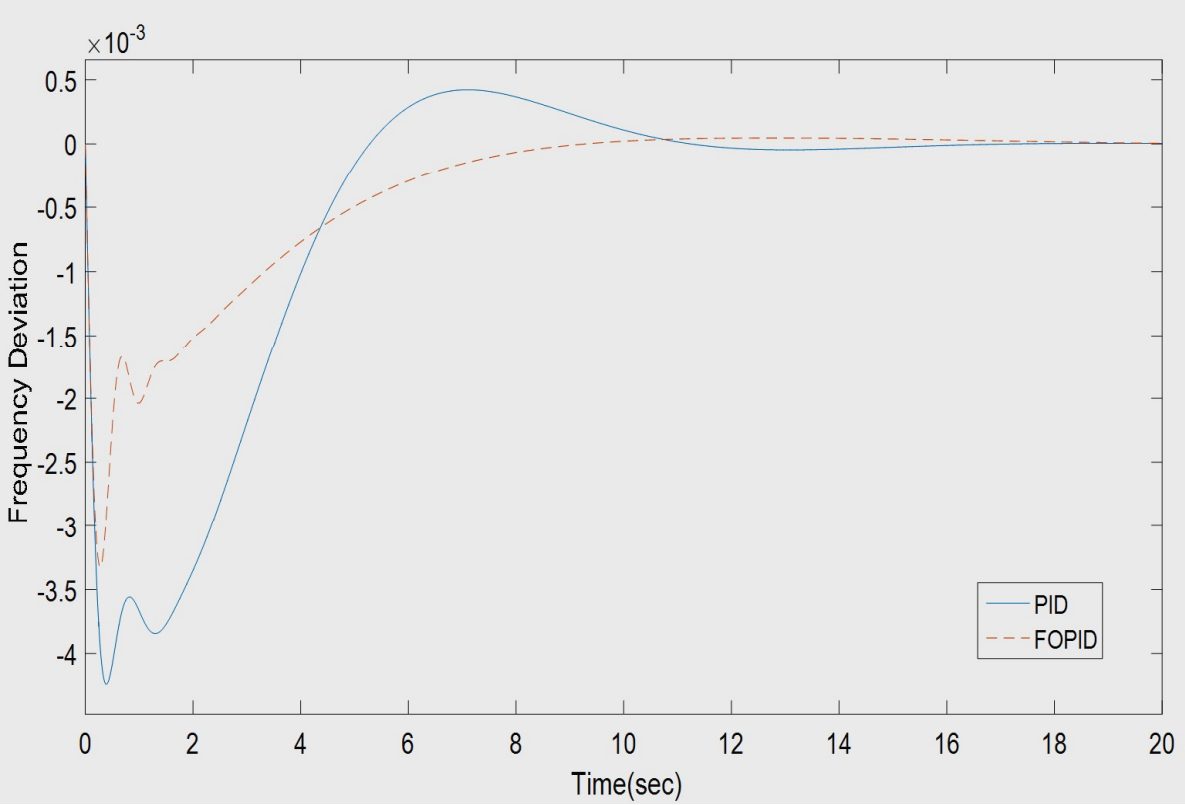

Figure 2.5. Response of AGC of IOPID and DBFOPID of an isolated system

Furthermore, the response of the DBFOPID controller is compared with the conventional controller. The comparison results ratify that DBFOPID outranks the PID controller in its response, which is measured in terms of rise time, settling time and overshoot time evident from Figure 2.5. It is observed that rise time, settling time and overshoot are reduced by 37%, 24% and 15% respectively with the introduction of DBFOPID controller.

Table 2.2: Summary of rise time, overshoot and settling time of different cases of the isolated system

	K_p	K_i	K_d	λ	μ	**Rise time (s)**	**Overshoot (Hz)**	**Settling time (s)**
AGC of IOPID controller	18.54	39.21	14.98	1	1	0.404	0.00424	4.556
AGC of DBFOPID controller	23.03	52.59	67.84	0.8	0.9	0.281	0.00335	3.829

The robustness of the system is investigated with the help of sensitivity analysis. The response of the controller with respect to variation of H, τ_G and τ_T is evaluated and the corresponding rise time, overshoot and settling time can be observed from Figure 2.6- Figure 2.11. To study the significance of each parameter individually, other parameters are maintained uniform while inducing a variation in other parameters and the findings are presented in Table 2.2. From the attributes in Table 2.2, it can be observed that there is a linear correlation between each of the parameters to rise time, settling time and overshoot time. The obtained values after computations are noted in Table 2.3 and are observed that the impact of τ_G on rise time, settling time and overshoot time is relatively less compared to H and τ_T. However, with the variation in H, τ_G and τ_T, no significant deviation of rise time, settling time and overshoot time is observed, which explicates that controller with the proposed configuration is robust.

To study the sensitivity, three different scenarios are developed by maintaining the two of the parameters in inertia constant, governor time constant and turbine time constant in the individual cases and the corresponding values can be drawn from Figure 2.6.

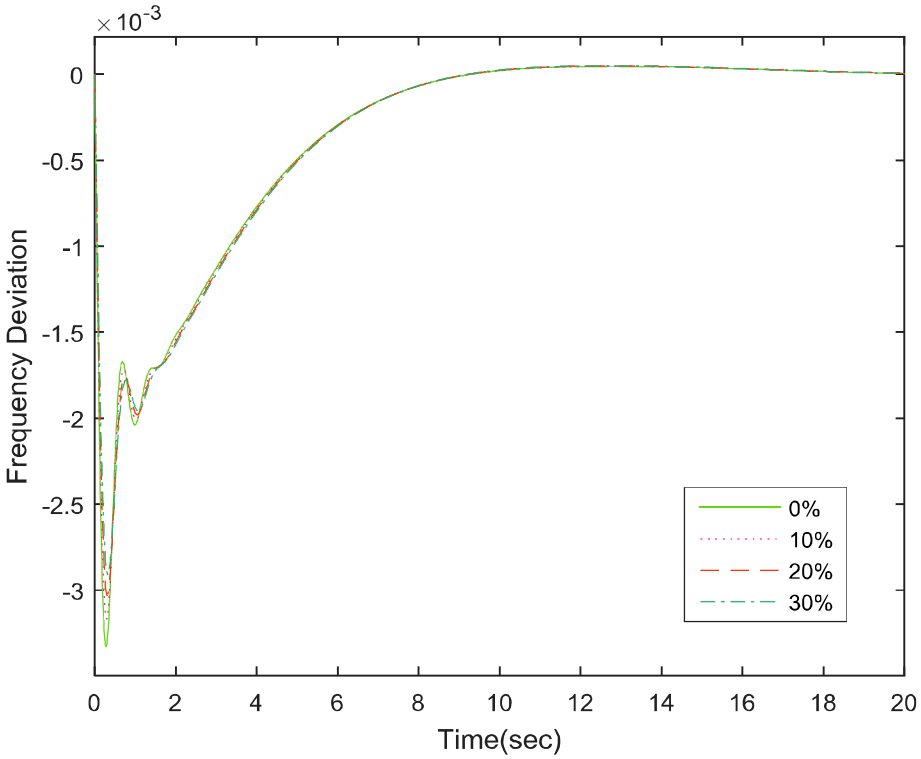

Figure 2.6. Response of AGC of DBFOPID by varying Inertia constant positively

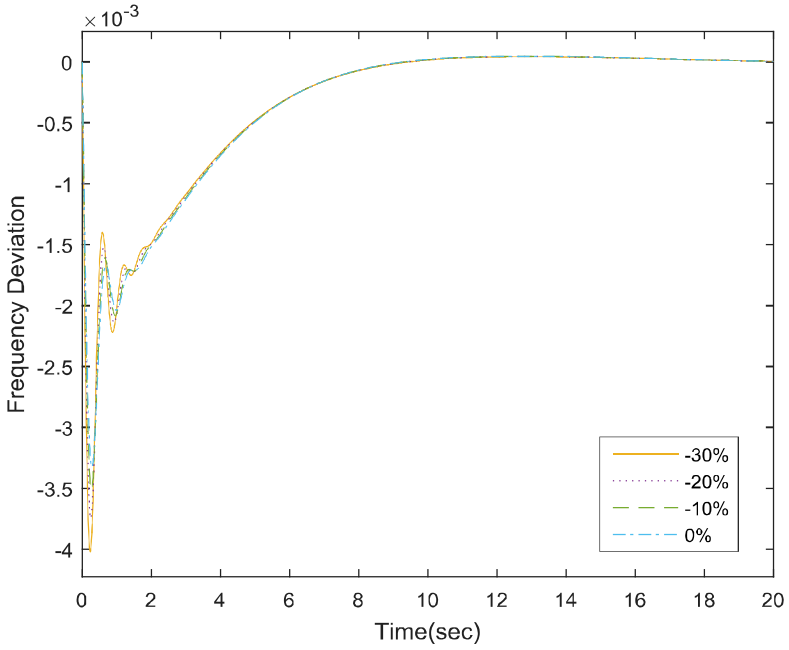

Figure 2.7. Response of AGC of DBFOPID by varying Inertia constant negatively

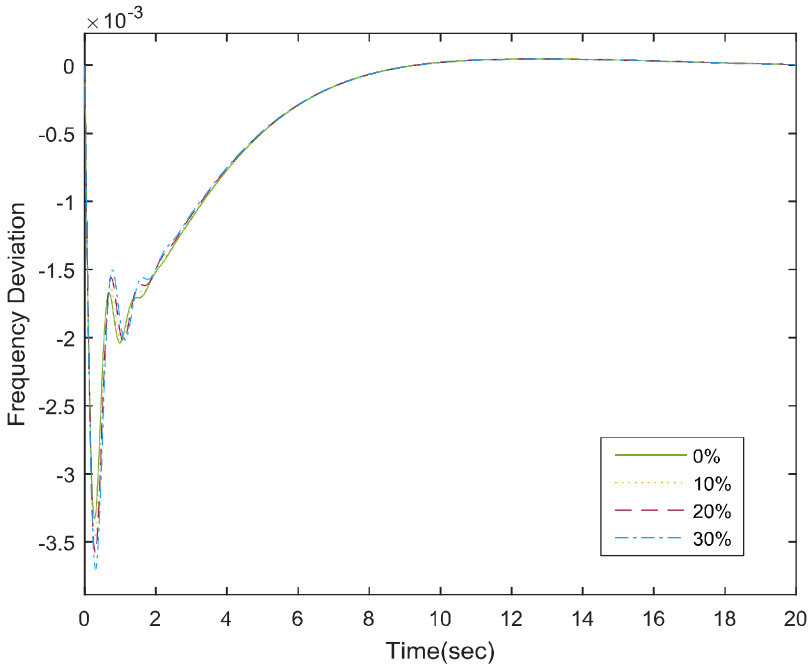

Figure 2.8. Response of AGC of DBFOPID by varying Inertia constant positively

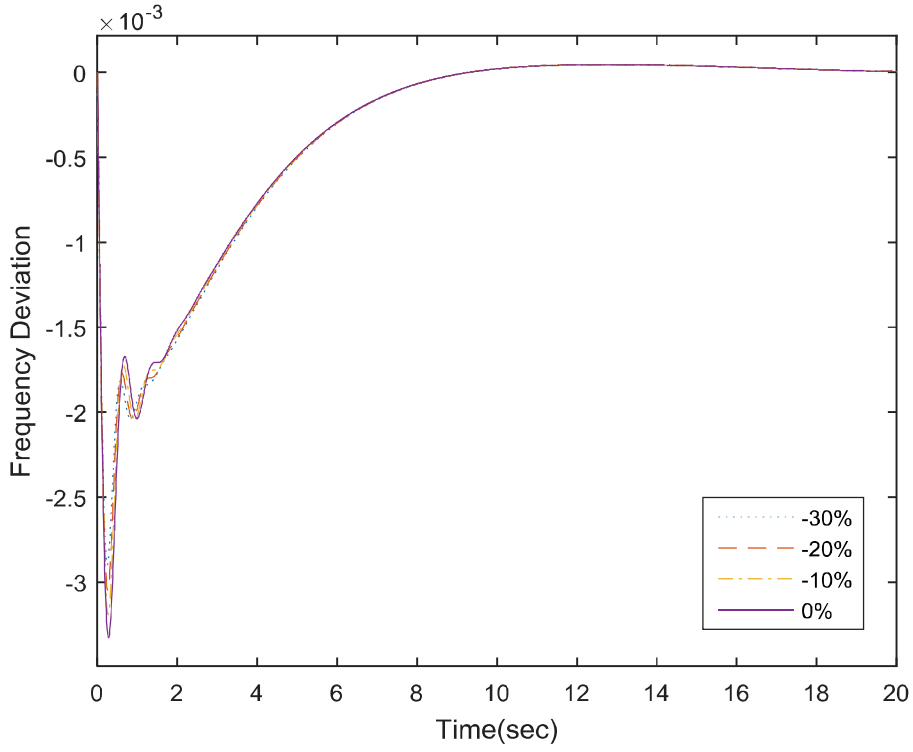

Figure 2.9. Response of AGC of DBFOPID by varying Governor time constant negatively

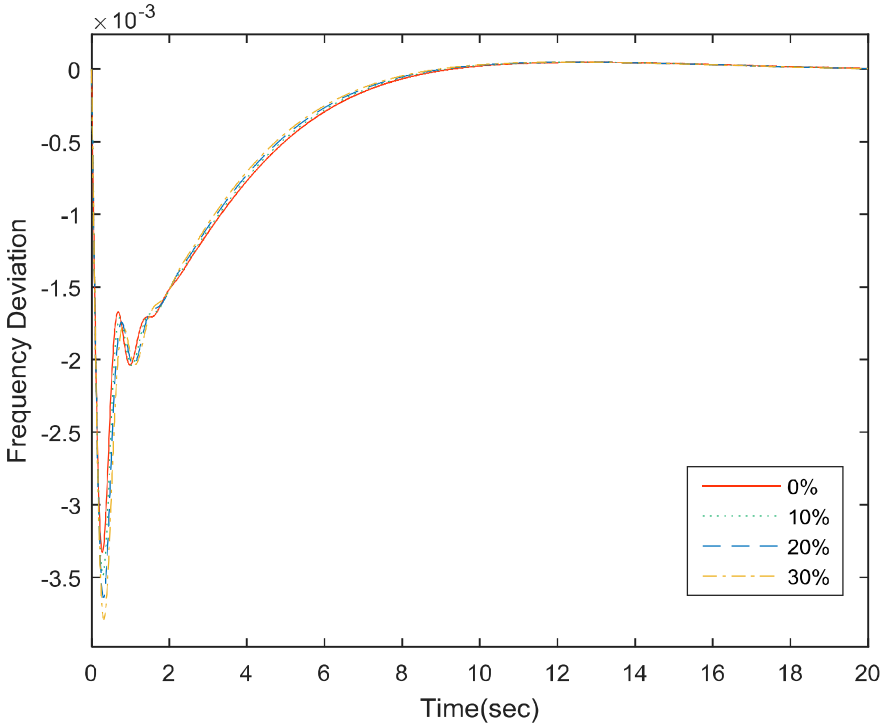

.

Figure 2.10. Response of AGC of DBFOPID by varying Turbine time constant positively

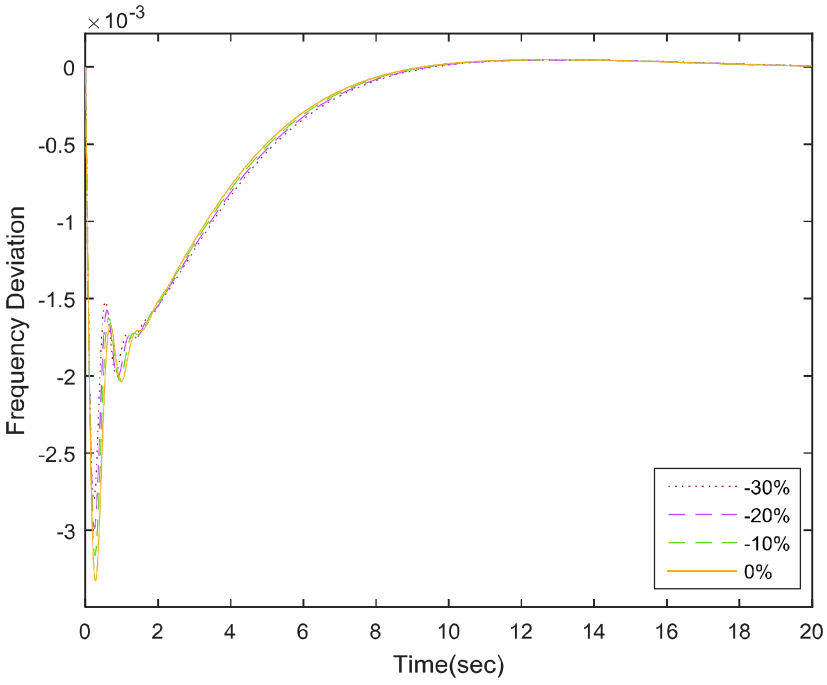

Figure 2.11: Response of AGC of DBFOPID by varying Turbine time constant negatively

The parameter which is maintained constant is varied up to 40% with an increment and decrement step size of 10%. This led to the 21 cases, which are categorized into three scenarios, namely

scenario 1, scenario 2 and scenario 3 as shown in Table 2.3. The responses of the controller in each of these cases are studied with the help of simulation. From the simulation results, no significant variations in the parametric values are observed. This can be interpreted with the fact that the variation in any of the parameters does not has any effect on the response of the system, which is measured in terms of overshoot, settling time and rise time. This interpretation can conclusively be used to state that the proposed system is robust.

2.9Model Description of AGC for Two Area System

The system frequency is controlled by AGC to enhance the quality of power supply in control systems. During normal operations in the two-area system, the real power is transferred to tie lines.

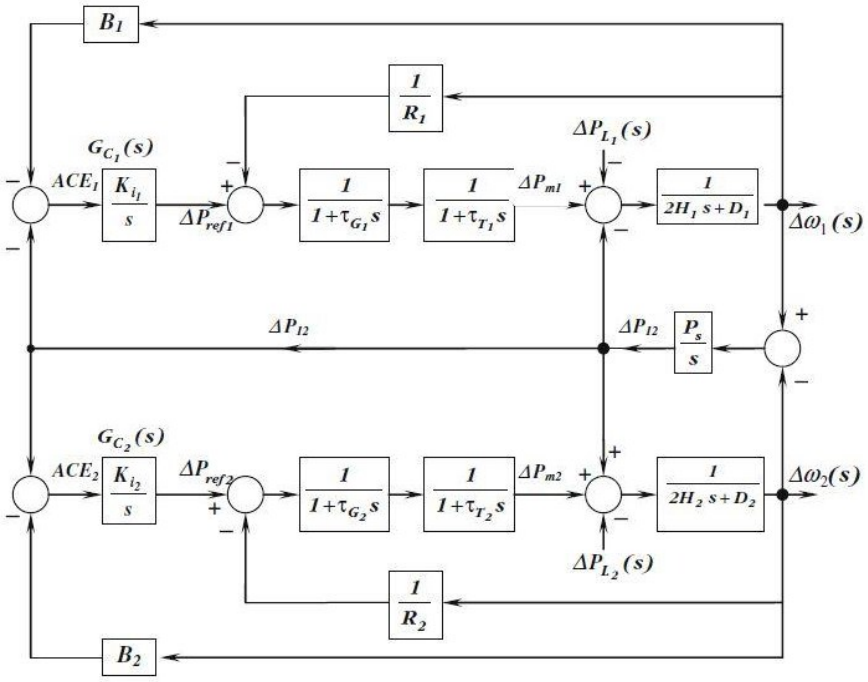

Figure 2.12. Block diagram of an AGC for two area system

The area control error (ACE) is a linear combination of the tie-line power flow changes and frequency deviation, which can be observed from Figure 2.12. Hence the ACE of area i is expressed as in (2.13):

$$ACE_i = \sum_{j=1}^{N} \Delta P_{ij} + B_i \Delta\omega_i \qquad (2.13)$$

Table 2.3: Analysis of Inertia constant, Governor time constant and Turbine constant

	(H, τ_G, τ_T)	Min	Max	Mean	Median	Mode	St. Dev	Rise time	Overshoot	Settling time
scenario 1	(3.5,0.2,0.5)	-0.00398	6.98	29	7.45	-0.00398	6.11	0.229	0.00398	3.791
	(4,0.2,0.5)	-0.00373	7.56	29	3.53	-0.00373	6.04	0.246	0.00373	3.797
	(4.5,0.2,0.5)	-0.00352	8.17	29	-0.942	-0.00352	5.98	0.264	0.00352	3.811
	(5,0.2,0.5)	-0.00335	8.78	29	-6.39	-0.00335	5.93	0.281	0.00335	3.829
	(5.5,0.2,0.5)	-0.00320	9.41	29	-12.4	-0.00320	5.89	0.297	0.00320	3.844
	(6,0.2,0.5)	-0.00308	10.1	29	-19.6	-0.00308	5.86	0.316	0.00308	3.859
	(6.5,0.2,0.5)	-0.00297	10.8	29	-27.5	-0.00297	5.83	0.329	0.00297	3.874
scenario 2	(5,0.14,0.5)	-0.00292	9.03	29	-3.03	-0.00292	5.71	0.250	0.00292	3.896
	(5,0.16,0.5)	-0.00307	8.95	29	-4.20	-0.00307	5.78	0.259	0.00307	3.874
	(5,0.18,0.5)	-0.00322	8.87	29	-5.26	-0.00322	5.85	0.267	0.00322	3.852
	(5,0.2,0.5)	-0.00335	8.78	29	-6.39	-0.00335	5.93	0.281	0.00335	3.829
	(5,0.22,0.5)	-0.00348	8.68	29	-7.32	-0.00348	6.02	0.292	0.00348	3.807
	(5,0.24,0.5)	-0.00360	8.57	29	-8.35	-0.00360	6.11	0.300	0.00360	3.787
	(5,0.26,0.5)	-0.00372	8.44	29	-9.29	-0.00372	6.20	0.309	0.00372	3.764
scenario 3	(5,0.2,0.35)	-0.00283	8.72	29	4.47	-0.00283	5.48	0.233	0.00283	4.051
	(5,0.2,0.4)	-0.00301	8.72	29	0.902	-0.00301	5.62	0.251	0.00301	3.978
	(5,0.2,0.45)	-0.00318	8.74	29	-2.64	-0.00318	5.77	0.265	0.00318	3.904
	(5,0.2,0.5)	-0.00335	8.78	29	-6.39	-0.00335	5.93	0.281	0.00335	3.829
	(5,0.2,0.55)	-0.00351	8.84	29	-10.2	-0.00351	6.10	0.295	0.00351	3.799
	(5,0.2,0.6)	-0.00366	8.92	29	-13.9	-0.00366	6.27	0.308	0.00366	3.754
	(5,0.2,0.65)	-0.00381	9.04	29	-17.9	-0.00381	6.45	0.321	0.00380	3.677

Note: St. Dev=Standard Deviation; Min= Minimum; Max= Maximum

Here N indicates the number of areas interconnected with area i, ΔP_{ij} is the deviation of power interchange between areas i and j from the scheduled values ΔP_{ij}, $\Delta\omega_i$ is the deviation in frequency (speed) of area i, and B_i is the frequency bias factor of the area i, given by (2.14):

$$B_i = \frac{1}{R_i} + D_i \tag{2.14}$$

The ACE_i is utilized to activate changes in frequency set point of an area i, when steady-state is reached, $\Delta P_{ij} = \Delta\omega_i = 0$. Then the optimal values for DBFOPID controller constants K_p, K_i, K_d, λ and μ are obtained by solving the optimization problem (2.15):

Minimize $ITAE_1(K_{i_1}, K_{i_2}) + ITAE_2(K_{i_1}, K_{i_2})$

Subject to

$$\begin{aligned} K_{i_1}^{min} \le K_i \le K_{i_1}^{max} \\ K_{i_2}^{min} \le K_i \le K_{i_2}^{max} \end{aligned} \tag{2.15}$$

If the IOPI controllers shown in the figure are replaced by DBFOPID controllers whose transfer functions are given by $G_{c_1}(s) = K_{p_1} + \frac{K_{i_1}}{s^\lambda} + K_{d_1}^{\mu} s^{\mu}$ and $G_{c_2}(s) = K_{p_1} + \frac{K_{i_2}}{s^\lambda} + K_{d_2}^{\mu} s^{\mu}$, then the optimal value for DBFOPID controllers $K_{p_1}, K_{i_1}, K_{d_1}, \lambda_1, \mu_1, K_{p_2}, K_{i_2}, K_{d_2}, \lambda_2 and \mu_2$ and are obtained by solving the optimization problem (2.16**)**.

Minimize $ITAE_1(x) + ITAE_2(x)$

$$\begin{aligned} K_{p_1}^{min} \le K_{p_1} \le K_{p_1}^{max} \\ K_{p_2}^{min} \le K_{p_2} \le K_{p_2}^{max} \\ K_{i_1}^{min} \le K_{i_1} \le K_{i_1}^{max} \\ K_{i_2}^{min} \le K_{i_2} \le K_{i_2}^{max} \\ K_{d_1}^{min} < K_{d_1} < K_{d_1}^{max} \\ K_{d_2}^{min} \le K_{d_2} \le K_{d_2}^{max} \\ \lambda_1^{min} \le \lambda_1 \le \lambda_1^{max} \\ \lambda_2^{min} \le \lambda_2 \le \lambda_2^{max} \\ \mu_1^{min} \le \mu_1 \le \mu_1^{max} \\ \mu_2^{min} < \mu_2 < \mu_2^{max} \end{aligned} \tag{2.16}$$

where $x = [K_{p_1}, K_{i_1}, K_{d_1}, \lambda_1, \mu_1, K_{p_2}, K_{i_2}, K_{d_2}, \lambda_2, \mu_2]^T$

2.10 Response of Two Area AGC System

The simulation results of AGC of two area systems using both the IO controller and the DBFOPID controller are compared. ITAE is considered for optimizing the constraints and obtain the values of K_p, K_i, K_d, λ and μ. and their limits are as follows in (2.17)

$$0 \leq K_p, K_i, K_d \leq 50;\ 0 \leq \lambda, \mu \leq 2 \qquad (2.17)$$

AGC responses are considered with Load change $\Delta P = 0.2\ p.u.$ The multiple AGC's as shown in Figure, which are termed as primary and secondary AGC are compared with AGC's of DBFOPID controllers.

Table 2.4: Data of the isolated and two area system (Alomoush 2010)

Component		**Isolated system**	**Area 1**	**Area 2**
Speed regulation	R	0.05	0.05	0.0625
Damping coefficient	D	0.06	0.60	0.90
Inertia constant	H	5.00	5.00	4.00
Governor time constant	τ_G	0.20	0.20	0.30
Turbine time constant	τ_T	0.50	0.50	0.60
Base power (MWA)	S_B	1000	1000	1000
Load change (MW)	ΔP_L	200	200	0
Synchronizing power coefficient	P_S	-	2	2

From Table 2.3, the fluctuations of AGC's are substantial and this can be improved effectively by the replacement of DBFOPID controllers.

The obtained rise time, overshoot and settling time after the simulation is given in the following Table 2.5.

Table 2.5: Summary of rise time, overshoot and settling time of different cases of the two-area system

	AGC of IO controller	**AGC DBFOPID controller 1**	**AGC DBFOPID controller 2**
Rise time (s)	0.783	0.283	0.35
Overshoot	1.43	0.4672	0.6363
Settling time (s)	9.29	2.486	7.298

It is evident from the Table 2.5, the rise time, overshoots and settling time are less as compared to conventional IO controllers. The summary of the values of rise time, overshoots and settling time of different cases of isolated systems are noted in Table 2.5.

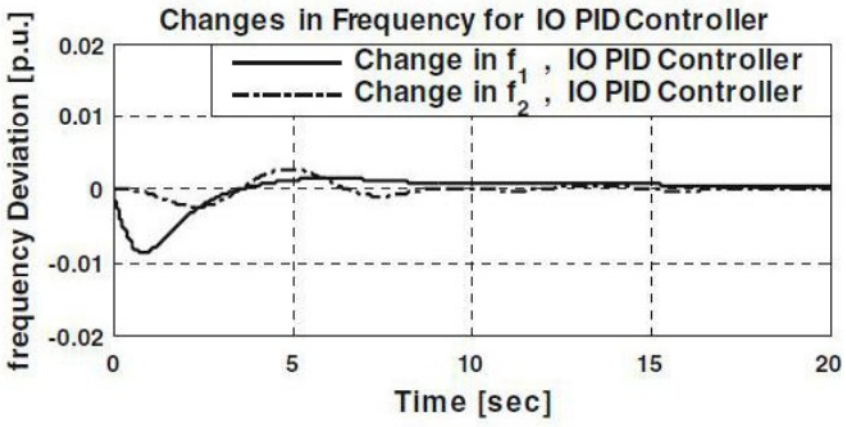

Figure 2.13. Response of AGC for two area system of IOPID controller

AGC of two area system by taking primary AGC responses are considered with Load change of $\Delta P_{L_1} = 0.2\, p.u.$ and $\Delta P_{L_2} = 0\, p.u.$ are shown in Figure 2.13. Figure 2.13 represents the frequency deviations of two area system with optimal PID controllers. If replaced by DBFOPID controllers, the responses are recorded as shown Figure 2.14.

The multiple AGC's, as shown in Figure 2.14, which is termed as primary and secondary AGC are compared with AGC's of DBFOPID controllers and the optimized parameters are given in Table 2.6.

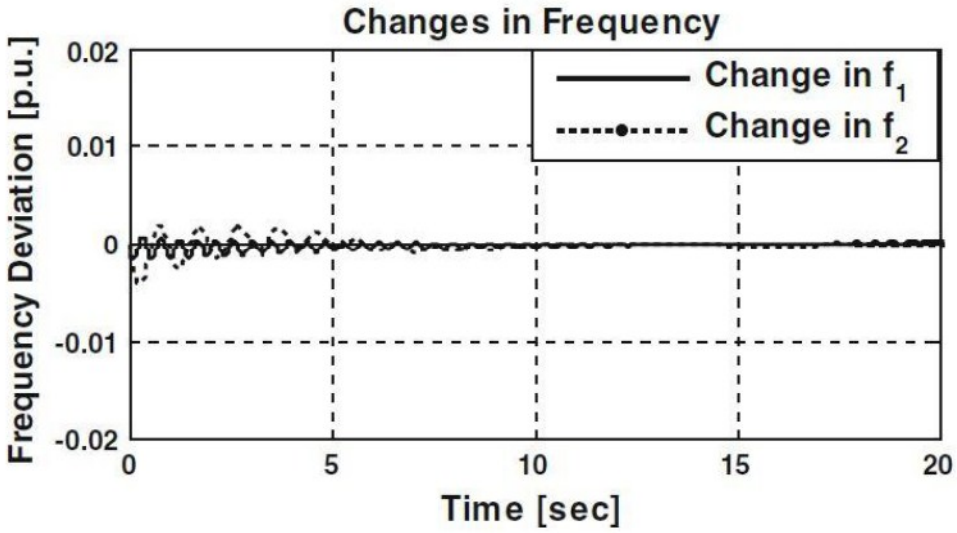

Figure 2.14. Response of AGC for two area system of DBFOPID controller

Table 2.6: Summary of rise time, overshoot and settling time of different cases of the two-area system

	PID controller 1	**PID controller 2**	**DBFOPID controller 1**	**DBFOPID controller 2**
K_p	0.0452	0.4121	4.6680	2.0013
K_i	0.4836	0.5027	9.7146	0.0000
K_d	004350	0.863	8.8890	22.921
λ	1	1	1.3004	1.5000
μ	1	1	0.7000	0.8000

2.11 Summary and Conclusions

A DBFOPID controller is proposed for AGC, and the characteristics of the system are studied for isolated and two-area power systems. The observed responses depict that the instabilities and fluctuations in the power system are slashed. It is also noted that the maximum deviation and settling time are reduced. Hence the DBFOPID, which has two additional tuning parameters compared to IOPID and dimensionally accurate compared to the FOPID controller, is more robust to IOPID controllers. The system remains robust even after altering parameters like Inertia constant, Governor time constant and Turbine time constant.

The literature reviewed; conclusively state that the dimensional aspects of FOPID controllers have been overlooked in the earlier research works. The findings of this study depict that the instabilities and fluctuations in the power system, which is evident from the frequency variations obtained. Further from the obtained results, it is observed that two area power system yields lower frequency deviations compared to an isolated system. This helps to derive that the optimal frequency deviations are directly proportional to the number of areas in the power systems. A similar response is observed in maximum deviation and settling time. DBFOPID has two additional tuning parameters compared to the PID controller and dimensionally accurate compared to the FOPID controller, which superior to PID controllers. From the comparative results, it can be stated that the system remains robust even after altering parameters like Inertia constant, Governor Time constant and Turbine time constant. The methodology proposed in this study can further be used to mitigate the frequency variation in power systems of multiple areas.